JOURNAL OF MATERIALS SCIENCE 19 (1984) 2805–2814

Strength degradation in SiC and Si_3N_4 ceramics by exposure to coal slags at high temperatures*

PAUL F. BECHER
Oak Ridge National Laboratory, Oak Ridge, Tennessee 37830, USA

Several commercial SiC and Si_3N_4 ceramics were exposed to the slag-like combustion products of coal–oil mixtures at approximately 1200° C to assess the effects of the ceramics composition on its corrosion behaviour and related changes in flexure strength including its temperature dependence. In the case of exposure to a slag from combustion of a basic coal–oil mixture, very accelerated corrosive attack occurs in both the SiC and Si_3N_4 ceramics such that the general rate of surface recession compared with localized corrosive attack limits the long-term load bearing capacity of the materials. Both the high-temperature corrosion for two different acidic slags and the resultant flexure strengths are dominated by either local enhanced surface corrosion (i.e. pitting) or slag penetration into the various materials which are strongly influenced by processing defects, impurities and/or second phases initially present in the ceramics. The SiC ceramics generally exhibited greater resistance to corrosive attack than did the Si_3N_4 ceramics.

1. Introduction

Conceptually ceramics could be utilized in heat exchanger systems involving the combustion of relatively dirty fuels such as residual fuel oils and/or coal or the recovery of waste heat [1, 2]. The mechanical and thermally induced tensile stresses imposed on the ceramics in such systems can be maintained at levels well below the fracture strengths of the commercially available products of the ceramics being considered. However, as previously discussed by Tennery and co-workers [3–5], the potential application of ceramics in such systems is very dependent upon their resistance to the corrosive environment produced during combustion.

The effects of corrosion via various sodium salts on SiC [6] and Si_3N_4 [7, 8] ceramics has been found to be a function of the salt/environment chemistry and the material composition. Similar effects were noted in coal slag environments for SiC ceramics [4, 5]. One concern in the use of ceramics in such environments is the influence of corrosion on the fracture strengths of such materials. As seen in previous oxidation studies [9], the retained strength of SiC ceramics is a function of the additives employed in and the impurities introduced during processing. In order to ascertain the effects of corrosive coal slags on the fracture strengths of ceramics, a study involving the exposure of several SiC and Si_3N_4 ceramics to coal slags at temperatures near 1200° C was undertaken.

2. Experimental procedures

The materials selected included hot pressed NC-132† and NCX-34† Si_3N_4 ceramics, hot pressed NC-203† SiC, sintered α-SiC (Hexalloy)‡ and siliconized KT SiC‡. Typical phases in the as-received materials as determined by X-ray diffraction analysis are shown in Table I. These materials were obtained in the form of rectangular cross section bars (typically 0.25 x 0.50 x 5 cm).

*Research sponsored by the US Department of Energy (DOE/PE AA 15 10 10 0, AR&TD Fossil Energy Materials Program, Work Breakdown Structure Element ORNL-5.12), under contract W-7405-eng-26 with the Union Carbide Corporation.

0022–2461/84 $03.00 + .12

TABLE I Phases present in as-received SiC and Si_3N_4 ceramics

	Major phases	Minor phases
SiC ceramics		
NC-203	α-SiC	WC
		α-Al_2O_3
Hexalloy	α-SiC	Si
KT	α-SiC	
	Si	
Si_3N_4 ceramics		
NC-132	β-Si_3N_4	WC
		Si_2ON_2
NCX-34	β-Si_3N_4	WC
		β-$Y_2Si_2O_7$
		unknown peaks

†Product of Norton Company, Worchester, MA, USA.
‡Product of Carborundum Corp., Niagara Falls, NY, USA.

The surfaces of the bars were finished and the edges bevelled by diamond grinding in a direction parallel to the length of the bar.

In the first series of mechanical tests, the fracture strengths of each material were determined in four point flexure (0.625 : 1.95 cm inner to outer spans) at 22° C (60% relative humidity air) at a stressing rate of 100 MPa sec^{-1}. Fracture strengths were obtained for samples in the as-received condition and after three different coal slag exposure conditions (CE-1, -2 and -3, described below). The second series of tests were similarly conducted on samples which had been exposed to one of the coal slag conditions (CE-1). In this case, samples were tested with 1 the glassy slag layer intact, and 2 after grinding off the glassy slag layer to expose the ceramic approximately 0.02 cm below the ceramic/slag interface. This was done to determine whether or not the corrosion involved primarily surface effects or altered the ceramic interior sufficiently to degrade the fracture strengths. The third series of tests measured the fracture strengths of the ceramics at temperatures of 1150 and 1300° C after the CE-3 exposure. This was done to ascertain if the post-exposure strengths varied significantly with temperature. This information would be necessary for ranking materials at potential use temperatures.

Samples were examined before and after exposure by a variety of techniques including X-ray diffraction analysis, scanning electron microscopy and complementary energy dispersive analysis and optical microscopy.

The exposure conditions, Table II, involved three separate combustion exposures (CE-1, -2 and -3) conducted in the ORNL Ceramic Recuperator Analysis Facility (CRAF, which is described elsewhere) [3, 4]. The CRAF system is basically a large combustion chamber in which the fuel consists of a mixture of No. 6 fuel oil and powdered coal. Combustion of the coal–oil mixture is assisted by first heating the combustion chamber to approximately 700° C by combustion of natural gas. The test samples were placed in siliconized KT SiC fixtures which were located in the exhaust flue of the CRAF. Sample temperatures were monitored by Pt against Pt–10% Rh thermocouples attached to the fixtures by a high purity

TABLE II Exposure conditions for the combustion exposure (CE) tests in the CRAF

	Exposure		
	CE-1	CE-2	CE-3
Sample temperature	1220° C	1220° C	1150° C
Time at temperature	500	240	350
Major oxide constituents in slag, wt%			
SiO_2	54	46	56
Fe_2O_3	21	11	4
Al_2O_3	19	14	31
CaO	0.1	19	0.5
MgO	0.9	7	0.8
Na_2O	0.6	1.1	2.5
K_2O	1.7	0.5	2.6
TiO_2	1.3	0.3	0.8
Ratio of basic oxides:			
Acidic oxides*	0.29	1.14	0.09
Nature of slag	porous solid	dense glass-like solid	low density particulate
Slag fusion temperature			

*Defined as Σ wt% (Fe_2O_3 + CaO + MgO + Na_2O + K_2O) to Σ wt% (SiO_2 + Al_2O_3 + TiO_2).

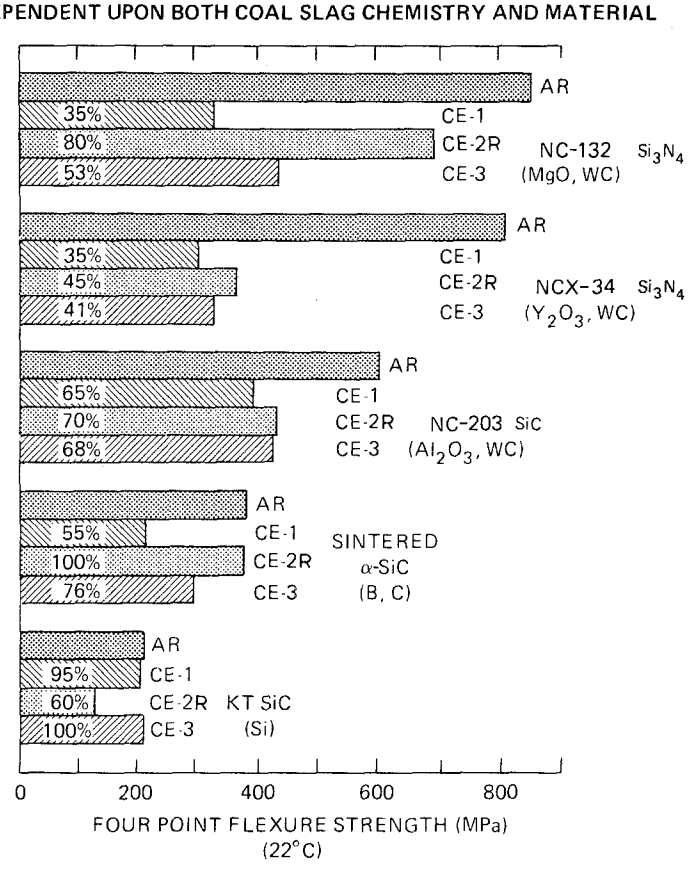

Figure 1 Fracture strengths of silicon based ceramics before (AR) and after high temperature exposure to various coal slags. Note the strength data for the CE-2 exposure are representative for samples exposed to the CE-2R coal slag in a laboratory tube furnace. Strengths of the sintered α-SiC and KT SiC samples recovered from the CE-2 exposure were ~ 75% and 60% of those of the as-received materials. Percentages of as-received strengths retained after CE exposures are also indicated.

alumina cement which also served to protect the thermocouples from the environment.

The coals employed were varied to obtain different coal slag chemistries, as seen in Table II. These three coals resulted in slags with different ratios of basic oxides to acidic oxides as well as slag viscosities at the combustion temperatures. A simulation of the basic coal slag exposure in CE-2 was conducted by coating samples with pulverized slag from the CE-2 run and exposing the samples to a flowing oxygen atmosphere in an alumina tube furnace at 1225° C for approximately 240 h. This laboratory simulation (designated CE-2R) was necessary due to the extremely excessive corrosion rates experienced in CE-2 and the attendant loss of many test specimen. In fact, only two sintered α-SiC and one KT SiC specimen of sufficient size for mechanical testing were recovered from the CE-2 exposure. While this simulated repeat of CE-2 does not exactly duplicate the dynamic corrosion environment in the CRAF where the slag is continuously replenished, it does allow one to examine the slag's corrosive effects on mechanical properties.

3. Results and discussion

3.1. Influence of coal slag on strength degradation

The fracture strengths of the ceramics at 22° C before and after exposure to the slags formed in CE-1, -2 and -3 are shown in Fig. 1. Note that the KT SiC fracture strengths were not influenced by exposure to the acidic slags in CE-1 and -3. It appears that the sintered α-SiC (Hexalloy) is unaltered by the basic slag in the simulated CE-2R exposure. However, unlike the KT SiC strengths noted above, there is a significant increase (two-fold) in the standard deviation of the sintered α-SiC strengths after the simulated CE-2R exposure. Sintered α-SiC samples recovered from the CE-2 exposure from the CRAF test exhibit a 25% loss in strength which compares very well with the average strength minus one standard deviation level obtained in the simulated CE-2R run.

In all other materials and test conditions there are significant losses in strength after the slag exposures. One can see that the extent of strength degradation for the NCX-34 Si_3N_4 and NC-203 SiC ceramics is comparable in either the acidic

TABLE III Phases present in the SiC and Si_3N_4 ceramics after exposure to the acidic slag in CE-1

Material	Interior surface ~ 0.02 cm below ceramic/slag interface	Ceramic/slag interface	Surface of glassy slag layer
Siliconized KT SiC	α-SiC Si	α-SiC SiC cristobalite	α-SiC cristobalite (increase)*
Sintered α-SiC	α-SiC	α-SiC cristobalite	α-SiC cristobalite (increase)*
NC-203 SiC	α-SiC WC α-Al_2O_3	α-SiC WC cristobalite	α-SiC WC cristobalite (increase)*
NC-132 Si_3N_4	α-Si_3N_4 WC Si_2ON_2 cristobalite	α-Si_3N_4 WC Si_2ON_2 (increase)* cristobalite (increase)*	α-Si_3N_4 WC Si_2ON_2 (increase)* cristobalite (increase)*
NCX-34 Si_3N_4	α-Si_3N_4 WC β-$Y_2Si_2O_7$ $Y_5Si_3O_{12}N$ cristobalite	α-Si_3N_4 WC β-$Y_2Si_2O_7$ $Y_5Si_3O_{12}N$ cristobalite (increase)* $RY_5Si_6O_{21}$† Y_2SiO_5	α-Si_3N_4 WC β-$Y_2Si_2O_7$ cristobalite (increase)* $RY_5Si_6O_{21}$† (increase)* Y_2SiO_5

*Increasing peak intensity with respect to underlying surface (i.e. amount of cristobalite increases going from interior surface to glassy slag layer in NCX-34 Si_3N_4.
†$RY_5Si_6O_{21}$, where R represents H, Na, Mn, Fe, Al, Th and Zr [13].

(CE-1 and -3) and the basic (CE-2R) slag exposures. In the case of the NCX-34 Si_3N_4, the slag corrosion always leads to slag penetration well into the Si_3N_4 ceramic. X-ray diffraction analysis shows that the slag corrosion is accompanied by formation of $Y_5Si_3O_{12}N$, Y_2SiO_5, cristobalite and $RY_5Si_6O_2$, in the region below and at the slag/ceramic interface, (e.g. Table III). The oxidation of $Y_5Si_3O_{12}N$ to form cristobalite (SiO_2) and $Y_2Si_2O_7$ and/or $RY_5Si_6O_{21}$ would involve a significant molar volume increase and subject the Si_3N_4 matrix to tensile stresses in the region of such reactions. Post-exposure microstructural observations reveal the formation of additional yttrium bearing phases and associated microcracking of the matrix, Fig. 2. The slag penetration thus is assisted by such microcracking and results in the strength degradations observed after the various slag exposures. As noted by previous studies [10–12], the cracking phenomena associated with the oxidation of Si_3N_4 ceramics employing a Y_2O_3 densification additive are sensitive to the Y_2O_3:SiO_2 ratios in the Si_3N_4 powders prior to densification. Materials fabricated with compositions within the Si_3N_4–Si_2ON_2–$Y_2Si_2O_7$ region of the Si_3N_4–SiO_2–Y_2O_3 ternary are not susceptible to such oxidation induced microcracking. However, the formation of complex yttrium–silicon–oxynitrides leads to cracking during oxidation and slag exposures.

The consistent strength losses in the NC-203 SiC after each slag exposure condition are associated with localized slag attack and formation of large subsurface pits, Fig. 3. These pits consistently acted as the source of failure in the exposed samples and are similar to those observed after oxidation of this material at 1200° C in a flowing oxygen environment [9]. As with the oxidation studies [9], the pit formation due to the coal slag exposures is associated with a grain boundary phase in the SiC. Note that there is also clear evidence for gas bubble formation in the slag adjacent to such pits, indicative of accelerated oxidation of the SiC to form volatile SiO and

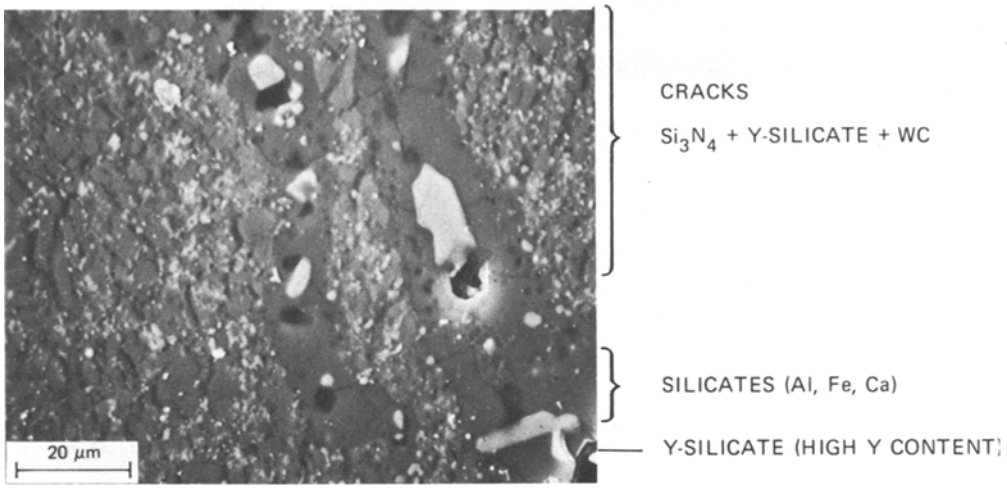

Figure 2 Microcracking and slag penetration associated with internal oxidation/reaction of yttrium bearing silicates (e.g. $Y_5Si_3O_{12}N$) in Si_3N_4 (NCX-34). Typical of behaviour observed after explosure to acidic and basic coal slags.

CO species. The presence of the alumina in SiC is found to promote the formation of fluid silicate boundary phases within the SiC [14] which can locally accelerate the oxidation of the SiC [9, 14]. The fact that the pit formation is relatively insensitive to the slag chemistry indicates that the impurities or additives present in the as-received NC-203 SiC dominate the local pitting phenomena. However, as discussed later, slag chemistry does influence the surface overall recession (corrosion) rates.

The strength losses in the NC-132 Si_3N_4 ceramics after the slag exposures also involve the formation of large, isolated surface/subsurface pits. Similar behaviour is observed in this material

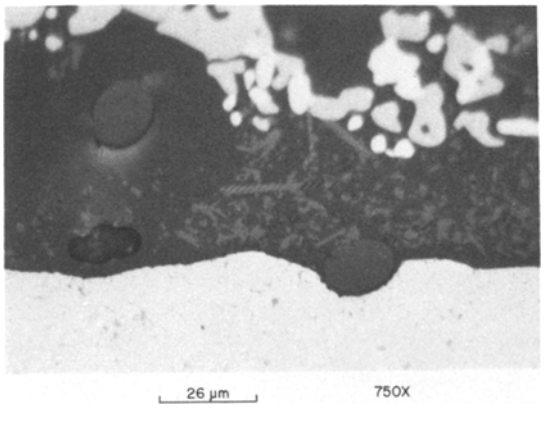

Figure 3 Pit formation and gas evolution in SiC ceramic (NC-203) which initially contains Al_2O_3 and WC internal phases. Coal slag chemistry does not appear to alter the nature of defects generated during corrosion.

after oxidation [15]. No such defects are observed in the as-received material; however, the presence of non-uniform distributions of the MgO additive may lead to local formation of Mg_2SiO_4. This phase is felt to lead to a low melting eutectic with Si_3N_4 and be responsible for the high temperature strength loss of Si_3N_4 having compositions near the Si_3N_4–Mg_2SiO_4 tie line on the Si_3N_4–SiO_2–MgO ternary [16]. As in the case of the NC-203 SiC [14], formation of a liquid or viscous silicates layer rather than a stable SiO_2 film would accelerate the oxidation/corrosion of the Si_3N_4. Owing to the local nature of such corrosive action one must also consider that local decreases in density may also influence the local acceleration of corrosion. Such local variations in density are not uncommon in ceramic bodies.

The sintered α-SiC (Hexalloy) ceramics exhibit uniform surface attack after the various coal slag exposures, Fig. 4. There are local regions where very subtle surface depressions occur (of the order of 10 μm deep by 30 μm wide). These would not appear to act as sufficient stress concentrations to lower the strengths to the observed levels. In previous oxidation studies where increases in strength were observed [9], internal lenticular defects were observed to act as the fracture origins, and when these were linked to the surface they contained oxidation products. Such defects are also observed to be fracture sources in the samples exposed to the coal slags. In these cases slag penetration into the defects and formation of additional phases on the internal surfaces of the

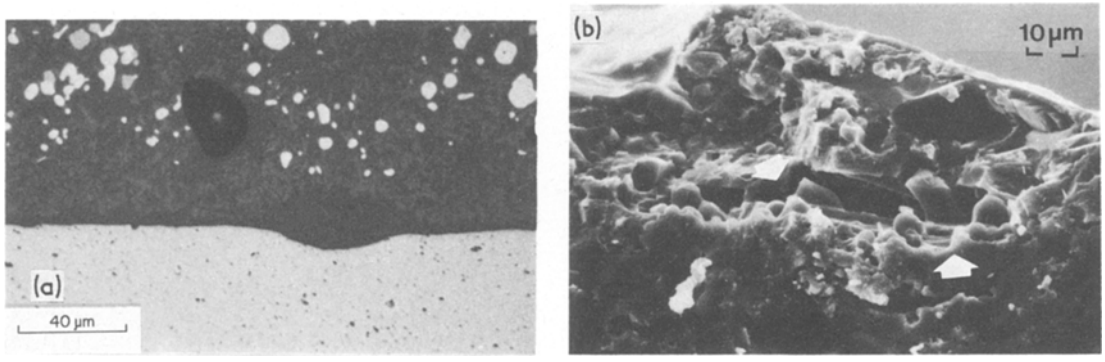

Figure 4 Corrosion of sintered α-SiC involves surface and connected defects. In either basic or acidic coal slags, the surface corrosion appears quite uniform with only occasional and very slight deviations in the corrosion interface, (a). Slag penetration into surface connected defects and subsequent development of reaction products (arrows) within these defects is also observed, (b).

defects were observed, Fig. 4. Aside from these observations, scanning electron microscope (SEM) observations of the surface of the sintered α-SiC after removal of the slag layer revealed that only very small ($\leqslant 1\,\mu m$) diameter voids are formed in the SiC surface. Note discrete regions ($\leqslant 1$ to $2\,\mu m$ in size) containing carbon are observed in the as-received material by transmission electron microscopy (TEM) [17] and free silicon can be occasionally detected via X-ray diffraction. The oxidation of these small carbon containing regions may be the source of the small surface voids. However, it appears that stresses generated by the slag penetration into the large lenticular defects lead to the strength loss observed in the sintered α-SiC ceramic as no change in defect geometry or type is observed.

Finally, the siliconized KT SiC after the acidic slag exposures exhibits neither a strength loss nor localized corrosion. In fact, the samples exposed to the acidic slags have quite smooth surfaces with negligible differences in surface recession between the SiC and Si phases, Fig. 5. Note in these cases there is some evidence of a thin second phase on the surfaces of the SiC grains. Similar layers on the silicon are not readily detectable, Fig. 5a. Under oxidizing conditions, the formation of a SiO_2 layer over the entire KT SiC surface is observed [9] and this plus the X-ray data in Table III suggest that a continuous SiO_2 layer is formed in the case of acidic slag exposures.

However, with the basic slag there is considerable loss in strength due to local penetration into the silicon phase of the KT SiC, Fig. 5b. As noted by McKee and Chatterji [6], the presence of basic salts can dramatically increase the corrosion rates

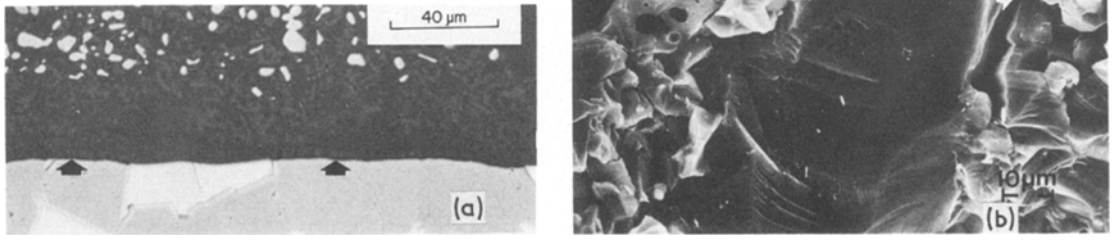

Figure 5 Corrosion behaviour of siliconized SiC is sensitive to the coal slag chemistry. Acidic coal slags develop a uniform corrosion front, as seen in (a). Oxide scale is observed on SiC (arrow) but is not readily detected on silicon (white phase) after exposure to acidic coal slag. Penetration and corrosive attack within the silicon phase are observed in the presence of the basic coal slag, (b). Note crystals in large pore in silicon phase (arrow).

of SiC, which is confirmed in the faster surface recession rates in the basic against acidic coal slag exposures noted below. However, we do not observe enhanced "localized" corrosion of SiC phase here and in the other SiC ceramics in the case of the basic slag – only that the silicon phase is more rapidly attacked as compared to the SiC phase. Two routes for this to occur exist. First as the partial pressure of oxygen (P_{O_2}) decreases the SiO_2 layer on Si will dissociate to form volatile SiO at higher P_{O_2} than in the case of SiC [18]. Therefore, the current results indicate that the P_{O_2} levels in the case of the fluid basic slag are lower as compared to that achieved with either of the acidic slags. The very dense nature of the basic slag as compared to acidic slag would be expected to limit oxygen transport to the ceramic surface. In the case where the protective SiO_2 layer is less stable on the Si against the SiC, the penetration rates into the silicon by the slag would be greater than those into the SiC.

Secondly, at low P_{O_2} the reaction of silicon with iron and nickel sources found both in the siliconized SiC and the slag can lead to the formation of eutectics and local melting [19] within the silicon phase. Evidence for such is seen in the growth of crystals within pockets in the silicon phase, Fig. 5b; this could occur via crystallization of a melt. This reaction-melt process would promote slag reactions by the presence of liquid within the silicon and hence accelerate slag penetration into the silicon.

One aspect of the corrosion that was extremely sensitive to the coal slag chemistry was that of surface recession (corrosion) rates for samples exposed in the tests run in the CRAF. In the case of the two acidic slags (CE-1 and -3) the overall surface recession rates for all materials were $\leqslant 2 \times 10^{-4}$ mm h^{-1}. However, in the basic coal slag exposure (CE-2) the surface recession rates were $\leqslant 2 \times 10^{-2}$ mm h^{-1}. This is consistent with the accelerated corrosion of SiC in the presence of basic salts previously observed [6, 20, 21] due to the formation of soluble silicates or volatile SiO rather than stable SiO_2 surface layers. In fact, the reduction of dimensions of the silicon based ceramic components in the basic slag would limit their load bearing capability, whereas localized corrosion during the acidic slag exposure limits the strengths of all but the siliconized KT SiC ceramics at these temperatures (~ 1200° C).

3.2. Strength of the bulk ceramic after exposure to acidic slag

As we have seen, the basic coal slag corrosion causes rapid dimensional changes in these ceramics. Thus, for this slag chemistry and temperature the ceramics studied are not viable candidate materials. However, they have considerable potential for use in acidic slags – particularly at lower temperatures. One concern for their use in acidic slags is whether or not the bulk ceramic is sufficiently altered by the formation of additional phases to degrade the strength of the bulk material. This is highlighted by the formation of additional phases and slag penetration well into the Si_3N_4 ceramic produced by the addition of Y_2O_3. In order to ascertain whether or not there is significant diffusion/penetration into the other ceramics by species present in the acidic slag, samples of the remaining ceramics were tested after grinding off material to a depth of approximately 0.02 cm from the ceramic/slag interface. This was sufficient to remove the region containing surface pits, etc. The resulting strengths for samples tested after the acidic slag exposure in CE-1 are shown in Fig. 6 along with the as-received and exposed condition with the slag intact. As can be seen, the strengths of the bulk materials with the surface reaction layer removed are comparable to the as-received materials, indicating that bulk material is not substantially altered after the 500 h exposure.

X-ray diffraction analysis of the surface of the glassy slag layer, the slag/ceramic interface and the interior surface approximately 0.02 cm below the interface does reveal formation of additional phases within the interior of the Si_3N_4 ceramics as compared to the as-received material. It has already been shown that formation of additional phases causes considerable changes in the bulk of the NCX-34 Si_3N_4. However, the formation of cristobalite within the NC-132 Si_3N_4, Table III, has no effect on its bulk strength after the 500 h exposure, Fig. 6. One should be careful in extending this to longer exposures as the phase transformation in cristobalite with decreasing temperature can introduce stresses. Thus, there is a potential for microcracking associated with more extensive cristobalite formation at longer exposure times. On the other hand, the interior of the SiC ceramics appear fairly stable, Table III, and the strength limiting feature of these materials appears to be localized surface corrosion.

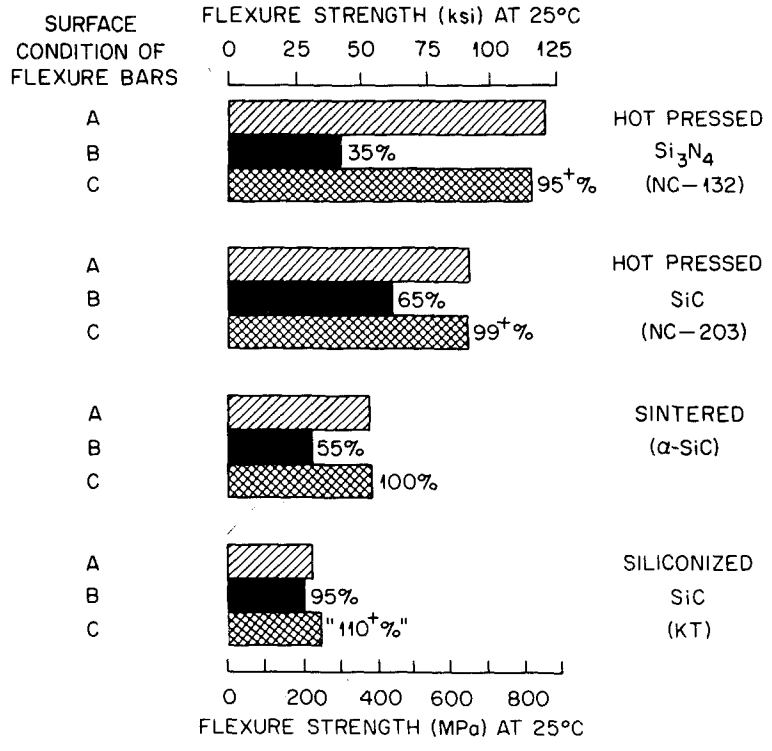

SURFACE CONDITION CODE:
A. AS-RECEIVED, DIAMOND GROUND
B. AFTER EXPOSURE IN CE-1
C. AFTER EXPOSURE IN CE-1 + DIAMOND GRINDING REMOVAL OF OXIDATION PRODUCT LAYER

Figure 6 Strength degradation of SiC and NC-132 Si_3N_4 ceramics is controlled by surface corrosion and not internal compositional or phase changes. Fracture strengths of samples exposed to acidic coal slag (CE-1) are identical to those of as-received samples when corroded surface of ceramic (~ 0.02 cm thick) is removed.

3.3. Influence of temperature on post-exposure (CE-3) strengths

As noted above, all the fracture strengths of the exposed samples were determined at room temperature. While these are important in determining the resistance of the various materials to the corrosive environments, they do not represent the strengths at the potential operating temperatures in heat exchangers or similar devices. Furthermore, any weakening of the ceramic due to internal reactions may best be reflected in their high temperature strengths. In order to determine such factors, samples from CE-3 were tested at 1150° C and 1300° C after exposure to the acidic slag. The three SiC ceramics were chosen for this study as they exhibited greater overall corrosion resistance and also include materials having different additives and impurities. As seen in Fig. 7, the high temperature strengths of the exposed SiC samples are not significantly different from those at room temperature. The strengths of the siliconized KT SiC are independent of test temperature up to 1300° C; this indicated that no additional weakening processes occur at elevated temperatures. The slight decrease in strength for the exposed NC-203 SiC at 1300° C is consistent with that observed in as-received NC-203 SiC tested in air [22], Fig. 7. Such behaviour is attributed to the presence of the grain boundary phase(s) observed in the material [9, 14]. Similar high temperature weakening is observed in Si_3N_4 fabricated with MgO additions as a result of the formation of viscous grain boundary phases with increasing temperatures [16].

The sintered α-SiC exhibits a general increase in strength with test temperature after exposure to the acidic slag (CE-3). In fact, at 1300° C the strengths of the as-received and as-exposed materials are comparable. This increase in strengths of the exposed samples with temperature increases suggests that, at high temperatures, relaxation of stresses associated with the slag and any reaction products formed within surface connected defects occurs. This is consistent with the observation that new major defects or pits are not formed as a result of the slag exposure and that strength

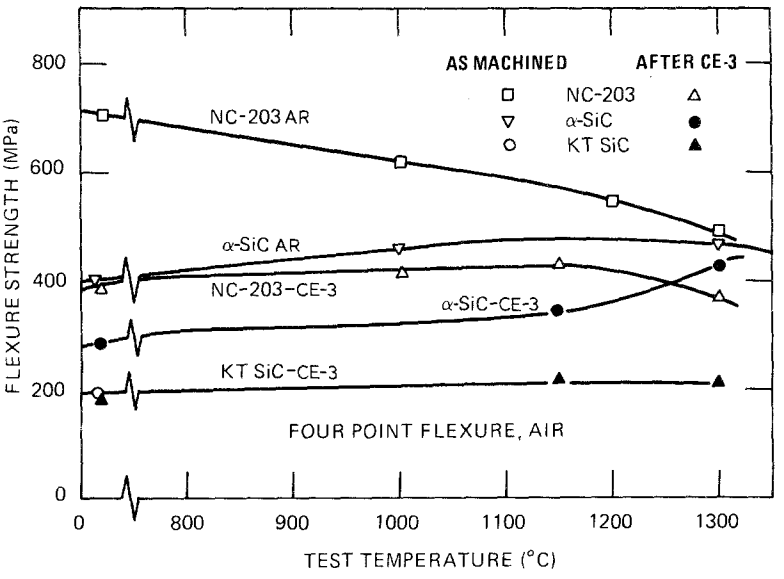

Figure 7 Fracture strengths of SiC ceramics exposed to acidic coal slag (CE-3) are influenced by test temperature. The exposed NC-203 SiC exhibits some loss in strength at elevated temperatures consistent with data for as-received (as-machined) material [22]. The sintered α-SiC ceramic after the CE-3 exposure shows a modest increase in strength with temperature. The siliconized SiC(KT) exposed in CE-3 exhibits no change in strength with temperature.

losses at room temperatures are a result of slag penetration into existing defects.

4. Summary

The potential application of silicon based ceramics in systems employing coal–oil mixtures is quite dependent on the chemistry of the coal slags (and operating temperature). The composition of the ceramic materials also plays an important role in their ability to withstand the corrosive environment. The basic coal slag studied here causes rapid material loss at the 1150° C exposure temperature. This feature is the overriding limitation for the use of such ceramics in this type of coal slag condition. These results, however, only provide guidance as to an upper temperature range where the ceramics are not applicable. At lower temperatures one expects the basic slag to be less aggressive in attacking the protective SiO_2 layer.

In acidic slag exposures, all the ceramics are more resistant to material removal by corrosion. The overall surface recession rates are decreased by at least two orders of magnitude compared to those after the basic slag exposure. Under such conditions, localized corrosion and the degrading effects on fracture strength will be the limiting characteristic for the application of such materials. In this case slag penetration and surface pitting due to corrosive reactions with the ceramics are dependent upon the composition of the ceramic.

The incorporation of Y_2O_3 in Si_3N_4 can lead to slag penetration by the matrix microcracking which results from the oxidation of, and reaction with, yttrium silicon oxynitride and yttrium silicate species. Surface/subsurface pitting occurs in the NC-203 SiC and the NC-132 Si_3N_4 and appears to be a result of reactions involving grain boundary phases present in the as-received materials. The strength loss at 22° C in sintered α-SiC behaviour is not a result of local accelerated surface corrosion and creation of new, large defects but is from the slag penetration into large existing delaminations or agglomeration type defects which are connected to the surface. At 1300° C the strengths of the as-received and post CE-3 exposure samples are comparable, indicating that the slag within such defects softens stresses due to thermal expansion mismatch or reaction products are minimized. Thus, with elimination of such processing defects sintered α-SiC together with KT SiC are the most promising commercial materials in terms of resistance to acidic slags and retention of strength as neither material exhibits localized corrosion in acidic slags.

Acknowledgements

It is a pleasure to acknowledge the work of J. F. Willmering, W. W. Warwick, W. H. Farmer, H. W. Dunn and J. C. Ogle during portions of these experiments. Discussions with M. K. Ferber and V. J. Tennery during the course of the work were extremely valuable.

References

1. V. J. TENNERY and G. C. WEI, Recuperator Materials Technology Assessment, ORNL/TM-6227 (1978).

2. V. J. TENNERY, Economic Application, Design Analyses, and Materials Availability for Ceramic Heat Exchangers, ORNL/TM-7580 (1981).
3. V. J. TENNERY, G. C. WEI and M. K. FERBER, *Ceram. Eng. Sci. Proc.* **2** (1981) 1171.
4. M. K. FERBER and V. J. TENNERY, *Amer. Ceram. Soc. Bull.* **62** (1983) 236.
5. *Idem*, *ibid.* in press (1984).
6. D. W. McKEE and D. CHATTERJI, *J. Amer. Ceram. Soc.* **59** (1976) 441.
7. W. C. BOURNE and R. E. TRESSLER, *Amer. Ceram. Soc. Bull.* **59** (1980) 443.
8. R. E. TRESSLER, M. D. MEISER and T. M. YONUSHONIS, *J. Amer. Ceram. Soc.* **59** (1976) 278.
9. P. F. BECHER, *Comm. Amer. Ceram. Soc.* **66** (1983) C-120.
10. G. D. WEAVER and J. W. LUCEK, *Amer. Ceram. Soc. Bull.* **57** (1978) 1131, 1136.
11. F. F. LANGE, *ibid.* **59** (1980) 239, 249.
12. C. L. QUAKENBUSH and J. T. SMITH, *ibid.* **59** (1980) 533.
13. J. ITO and H. JOHNSON, *Amer. Mineral.* **53**, (1968) 1940.
14. S. C. SINGHAL and F. F. LANGE, *J. Amer. Ceram. Soc.* **58** (1975) 433.
15. S. W. FREIMAN, A. WILLIAMS, J. J. MECHOLSLEY and R. W. RICE, in "Ceramic Microstructures", edited by R. M. Fulrath and J. A. Pask (Westview Press, Boulder, CO, 1977) pp. 824–834.
16. R. J. BRATTON, C. A. ANDERSON and F. F. LANGE, in "Ceramics for High Performance Applications – II", edited by J. J. Burke, E. N. Lenoe and R. N. Katz (Brook Hill Publ. Co., Chestnut Hill, MA, 1978) pp. 805–825.
17. P. S. SKLAD, Oak Ridge National Laboratory, personal communication (1981).
18. E. A. GULBRANSEN and S. A. JANSSON, *Oxid. Met.* **4** (1972) 181.
19. M. HANSEN, "Constitution of Binary Alloys" (McGraw-Hill, New York, 1958).
20. G. ERVIN, Jr., *J. Amer. Ceram. Soc.* **41** (1958) 347.
21. E. BUCHNER and O. RUBISCH, in "Silicon Carbide – 1973", edited by R. C. Marshall, J. W. Faust and C. W. Ryan (University of South Carolina Press, Columbia, 1974) pp. 428–34.
22. D. C. LARSEN and J. W. ADAMS, Property Screening and Evaluation of Ceramic Turbine Materials, Semiannual Interim Technical Report No. 8, IIT Research Institute, Chicago, IL, June (1980).

Received 10 October
and accepted 26 October 1983